Materials Research Bulletin 125 (2020) 110806

Contents lists available at ScienceDirect

Materials Research Bulletin

journal homepage: www.elsevier.com/locate/matresbu

Room-temperature preparation of MIL-88A as a heterogeneous photo-Fenton catalyst for degradation of rhodamine B and bisphenol a under visible light

Huifen Fu, Xiao-Xu Song, Lin Wu, Chen Zhao, Peng Wang, Chong-Chen Wang*

Beijing Key Laboratory of Functional Materials for Building Structure and Environment Remediation/Beijing Advanced Innovation Centre for Future Urban Design, Beijing University of Civil Engineering and Architecture, Beijing, 100044, China

ARTICLE INFO

Keywords:
MOF
MIL-88A
Room-temperature preparation
Photo-Fenton
Visible light

ABSTRACT

MIL-88A, a Fe-based MOF, with different sizes was prepared successfully at room-temperature, which was characterized by scanning electron microscopy (SEM), X-ray diffraction (XRD), Fourier transform infrared spectroscopy (FTIR) and UV–vis diffuse reflectance spectroscopy (UV–vis DRS). Water played an important role in the room-temperature synthesis as water could facilitate the deprotonation of fumaric acid and hydrolysis of iron salt to accelerate crystal nucleation, and this room-temperature preparation is beneficial to the large-scale synthesis and is imperative to push forward the development of the MIL-88A. The as-prepared MIL-88A exhibited excellent photo-Fenton catalytic performance towards rhodamine B and bisphenol A removal under visible light irradiation (LED). The main active specie was investigated, the degradation mechanism and BPA degradation pathway were proposed. Furthermore, the as-prepared MIL-88A displayed good reusability, and there was no obvious decline of degradation performance after five cycles.

1. Introduction

Organic dyes and pharmaceuticals and personal care products (PPCPs) are typical organic pollutants in water pollution, which pose risks to the ecological environment and human health [1,2]. It is reported that organic pollutants, including dyes and PPCPs, widely existed in surface water, ground water, and even drinking water due to their widespread use. Currently, various methods have been applied to the treatment of organic pollutants in water, such as adsorption [3,4], biodegradation [5], photocatalysis [6–8], advanced oxidation processes (AOPs) [9–12] and so on. Among these methods, AOPs is considered to be a promising technology for organic contaminants removal.

Metal-organic frameworks (MOFs), an emerging porous crystalline material constructed from metal and organic linker, with the merits of large surface area and tunable pore size, received widespread attention in many fields, such as sensor, [13–15] gas storage [16,17], gas separation,17,18] adsorption, [19–21] electrochemistry [22], catalysis [23], and photocatalysis [24,25]. Fe-based MOF, as a heterogeneous photo-Fenton materials, has been widely investigated [26]. Liang and coworkers prepared Pd@MIL-100(Fe) to accomplish outstanding photocatalytic activity for PPCPs (theophylline, ibuprofen and bisphenol) degradation with the help of H_2O_2 [27]. Li and coworkers prepared Fe_3O_4@MIL-100(Fe) that exhibited excellent removal efficient of diclofenac sodium via adsorption removal and the consequent photocatalytic degradation in the presence of H_2O_2 [28]. Recently, Fe-based MOFs, such as MIL-100 [29,30], MIL-101 [31,32], MIL-53 [33,34], MIL-88A [35], and MIL-88B [36,37] as visible-light-driven photocatalysts and photo-Fenton catalysts had attracted great attention. Among these Fe-based MOFs, MIL-88A, built from Fe^{3+} and fumaric acid, was a good candidate for the scale applications because of the low price.

Currently, there are a large number of MOFs being synthesized via solvothermal method [38,39]. However, much concerns should be put on the facile preparation method of MOFs, which can not only reduce energy consumption but also facilitate the development and application of the MOFs [40,41]. In this work, a room-temperature preparation method of MIL-88A was firstly reported, in which the sizes of MIL-88A can be easily controlled by changing the amounts of the reactants. The obtained MIL-88A presented excellent photo-Fenton degradation efficiency towards rhodamine B (RhB) and bisphenol A (BPA) under visible light irradiation. Furthermore, the MIL-88A can be recycled without obvious decrease of the degradation efficiency.

* Corresponding author.
E-mail address: chongchenwang@126.com (C.-C. Wang).

https://doi.org/10.1016/j.materresbull.2020.110806
Received 1 November 2019; Received in revised form 26 January 2020; Accepted 26 January 2020
Available online 27 January 2020

2. Experimental section

2.1. Reagents

Fumaric acid, bisphenol A (BPA) and isopropanol (IPA) was bought from J&K Scientific Ltd. $FeCl_3{\cdot}6H_2O$, ethylenediaminetetraacetic acid (EDTA) and terephthalic acid were bought from Sinopharm. Rhodamine B (RhB) was bought from Beichen Founder Reagent Factory. All the reagents were used directly without further treatment.

2.2. Preparation of MIL-88A

10 mmol fumaric acid and 10 mmol $FeCl_3{\cdot}6H_2O$ were dissolved in 75 mL ethanol and 75 mL ultrapure water, respectively. The two solutions were mixed, and stirred for 24 h at room temperature. The products (MIL-88A-1) were washed by ethanol and separated with the aid of centrifugation. As well, MIL-88A-2 was prepared using the similar method by replacing 10 mmol fumaric acid and 10 mmol $FeCl_3{\cdot}6H_2O$ with 20 mmol fumaric acid and 20 mmol $FeCl_3{\cdot}6H_2O$.

2.3. Characterization

X-ray diff ;raction (XRD) patterns were recorded on a Dandonghaoyuan DX-2700B diff ;ractometer using Cu Kα radiation. Hitachi SU8020 scanning electron microscope (SEM) was used to measure the morphology of the samples. UV–vis diffuse-reflectance spectra (UV–vis DRS) were obtained on a Perkin Elmer Lambda 650S spectrophotometer. Fluorescence spectra were conducted on a Hitachi F-7000 and Techcomp FL970 spectrophotometer in the range of $350-600$ nm.

2.4. Photo-Fenton catalytic experiment

10 mg MIL-88A-1 or MIL-88A-2 was dispersed in 50 mL 10 mg/L RhB (or BPA) solution with the help of ultrasound. After stirring under dark condition for 60 min, 100 μL 30 % H_2O_2 was added in, and soon the solution was irradiated by 350 mW LED visible light source (PCX50A, Beijing Perfect Light Technology Co., Ltd.). At a certain time interval, 1.5 mL solution was extracted from the reactor by a 0.22 μm filter, which was quenched with 20 μL IPA. UV–vis absorption spectroscopy was used to measure the residual RhB concentration. A UPLC (Waters) equipped with a TUV detector was used to determine the concentration of BPA. The analytes were separated by a C18 column (1.7 μm, 2.1 mm × 50 mm), and acetonitrile and water (V:V = 65:35) were used as mobile phase A and B, respectively. To understand the degradation pathway of BPA, A LC (Thermo scientific Vanquish) coupled with a MS (Q Exactive Focus) was used to identify the intermediates using a column (Hypersil Gold aQ, 100 × 2.1 mm, 1.9 μm).

3. Results and discussions

As reported, Fe^{3+} can react with fumaric acid to form MIL-88A at high temperature [42]. In our case, MIL-88A can be harvested via the reaction between aqueous solution of $FeCl_3$ and alcohol solution of fumaric acid at room temperature, which was affirmed by the XRD patterns, FTIR spectra and SEM images as illustrated in Fig. 1. It can be seen from Fig. 1a that the XRD characteristic diffraction peaks of the MIL-88A-1 and MIL-88A-2 matched well with those of the simulated one [43,44]. It was reported that guest molecule affected the XRD pattern of MIL-88A [45]. In our case, the MIL-88A was washed with ethanol twice in order to be dried within a short time. As shown in Fig. S1, the XRD pattern of MIL-88A washed with ethanol is different from that washed with water, and the main difference was the intensities of peaks at about 10.8° and 12°. The intensity of the former peak was higher than that of the later one when ethanol as washing solvent, while the later peak was higher than that of the former one when water as washing solvent. When the product was firstly washed with water and then washed with ethanol, the intensities of the two peaks are similar (Fig. S1). Because the MIL-88A washed with water is difficult to be dried, ethanol was used as washing solvent during the preparation process in order to obtained the MIL-88A within a short time.

SEM images (Fig. 1b and c) show that the obtained MIL-88A present spindle-like shape, and the length and width of MIL-88A-1 were about 1000 and 500 nm, respectively, while 500 and 300 nm for the MIL-88A-2, respectively, indicating that reactant concentration exerts no influence to the morphology. However, high concentrations of the reactants facilitate to reduce the particle size of MIL-88A, which corresponds well with the previous literature [46]. FTIR spectra were also conducted, as shown in Fig. 1d. The bands at 1396 and 1603 cm^{-1} can be attributed to the symmetric and asymmetric vibration of the carboxyl group ($-COOH$), respectively [47,48]. The band at 672 cm^{-1} can be assigned to vibration mode of Fe-O [47].

It is worthy to note that no obvious precipitation was seen by naked eyes when ethanol was used as the sole solvent while brick-red products were precipitated immediately in the presence of water, indicating that water played an important role in the room-temperature preparation process. It is speculated that H_2O could accelerate deprotonation of fumaric acid and hydrolysis of iron salt to promote crystal nucleation of MIL-88A, as reported in the literature [49]. Wang's group [50] found that zirconium- and hafnium -based MOF nanocrystals were synthesized under mild condition in the presence of water and acetic acid. As far as we know, it is the first report of the room-temperature preparation of MIL-88A. This room-temperature preparation method is green as just water and ethanol were used as solvents, and the large-scale synthesis can be easily realized by using larger reactor, which is beneficial to scale application of MIL-88A.

UV-Vis DRS (Fig. 2a) was used to characterize the optical absorption property of the MIL-88A. There are obvious absorption peaks at $200-600$ nm of the two samples, and E_g was approximately 2.02 eV (Fig. 2b), which is similar to the previous literature [51,52]. RhB was selected as the target pollutant to study the catalytic performance under visible light. As depicted in Fig. 3a, both MIL-88A-1 and MIL-88A-2 had little adsorption capacity toward RhB, and only approximately 10 % RhB adsorption was accomplished after 30 min under dark condition. It can be seen that mostly complete degradation of RhB was accomplished after 80 min and 60 min irradiation under visible light in the presence of H_2O_2 for the MIL-88A-1 and MIL-88A-2, respectively, indicating good visible-light-driven catalytic activity of the prepared MIL-88A. The catalytic activity of the MIL-88A-2 was better than that of the MIL-88A-1, which could be attributed to the smaller size and more active sites of the MIL-88A-2 [53].

To further confirm the as-synthesis MIL-88A with good visible-light-driven catalytic performance, control experiments were conducted. As shown in Fig. 3b, after 120 min irradiation under visible light, self-degradation of RhB was about 15 %, and only 21 % degradation were realized just with the addition of MIL-88A-2. RhB degradation with the oxidation of H_2O_2 under visible light was just 28 %. The RhB degradation was also conducted under dark condition in the presence of MIL-88A-2 and H_2O_2. The results show that the RhB degradation was also limited, and 37 % RhB degradation was accomplished, which could be ascribed to the effect of Fenton-like catalysis due to the existence of Fe-O clusters on the surface of MIL-88A. When both MIL-88A-2 and H_2O_2 were added under visible light, a markedly increase of the RhB degradation appeared. The Fe content measured by ICP-OES (ICP-5000, Focused Photonics (Hangzhou) Inc.) in the solution was 1.6 ppm after photodegradation, and it can be observed from Fig. S2 that the degradation efficiency of RhB was 58 % within 60 min in the presence of 1.6 ppm Fe^{3+} under visible light, which is far lower than that of the MIL-88A-2, implying the good catalytic degradation of MIL-88A-2 under visible light irradiation.

The initial concentration of target pollutants and H_2O_2 dosage are important parameters for the degradation of organic contaminants.

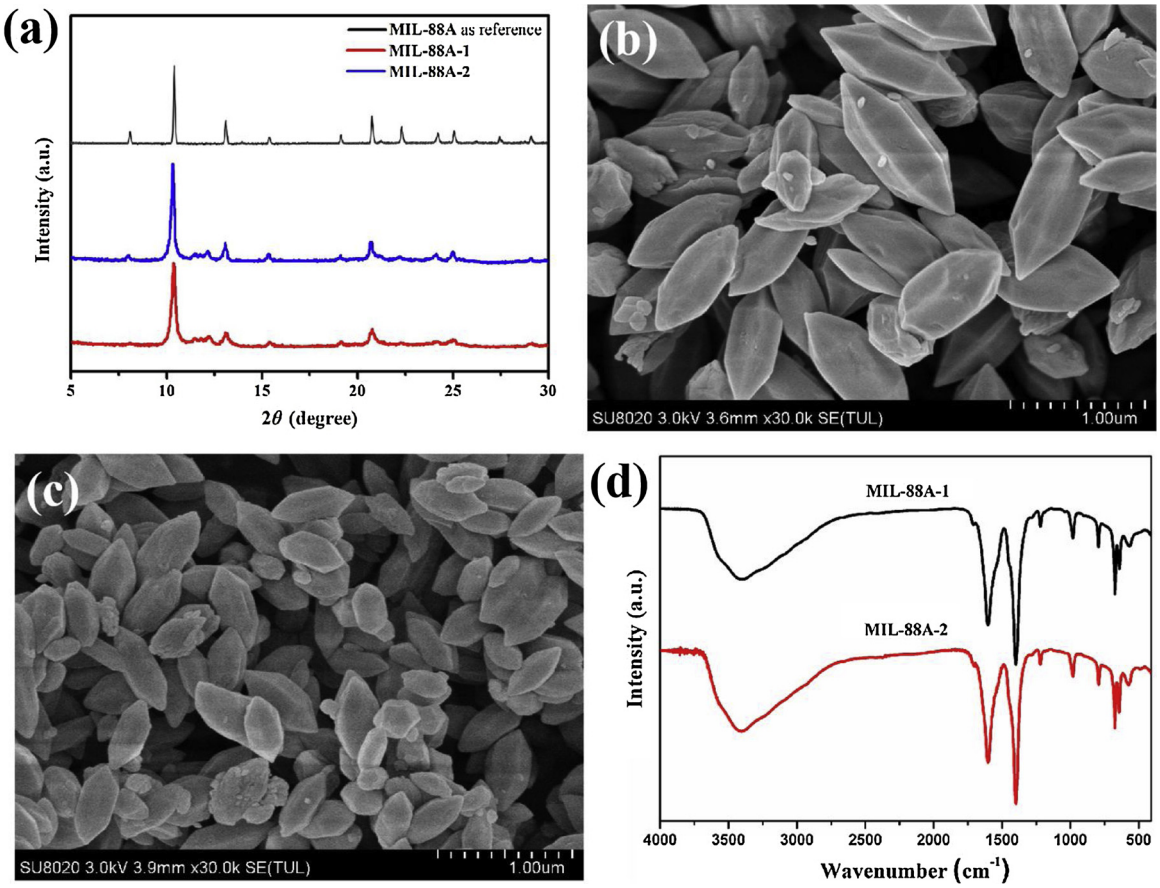

Fig. 1. (a)XRD patterns of simulated MIL-88A, MIL-88A-1 and MIL-88A-2, (b–c) SEM images of (b) MIL-88A-1 and (c) MIL-88A-2, (d) FTIR spectra of MIL-88A-1 and MIL-88A-2.

Therefore, the effects of these factors on the RhB degradation were studied. Fig. 4a shows the degradation efficiency of various initial concentration of RhB ranging from 10 to 100 mg/L under visible light irradiation. It can be clearly seen that the almost completely degradation of RhB was accomplished after 60, 60 and 80 min irradiation when the initial concentration of RhB was 10, 20 and 50 mg/L, while just reached 95 % for 100 mg/L after 120 min irradiation, implying that the degradation efficiency decreased as the increasing of the RhB concentration. The effect of H_2O_2 dosage ranging from 50 − 200 μL on the RhB degradation efficiency was shown in Fig. 4b. The degradation efficiency of RhB was 92.5 %, 98.0 % and 99.4 % when the H_2O_2 dosage was 50, 100 and 200 μL, indicating that the increase of H_2O_2 dosage did not result in great enhancement of RhB degradation efficiency.

PPCPs, as a kind of emerging pollutants, pose serious threats to the ecological environment and even human health, and the control of PPCPs is of great significance. Therefore, BPA was also selected as target pollutant to study the catalytic performance of the as-synthesis MIL-88A. The results (Fig. 5a) show that MIL-88A-1 and MIL-88A-2 exhibited excellent catalytic activity towards BPA degradation, and the degradation of BPA was 95 % and 100 % for the MIL-88A-1 and MIL-88A-2, respectively after 80 min irradiation. It can be observed from Fig. 5a that the degradation efficiency of the MIL-88A-2 was better than

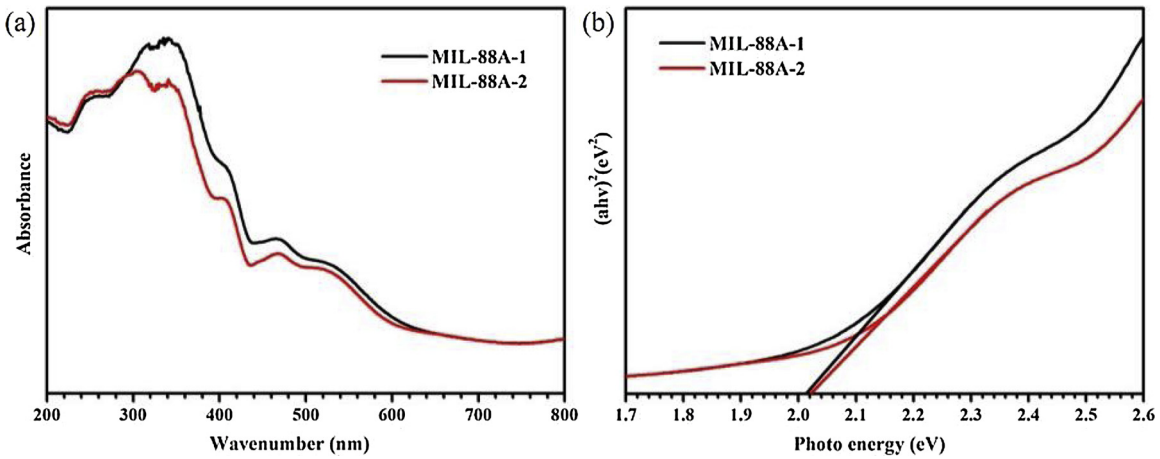

Fig. 2. (a) UV–vis DRS and (b) E_g plots of MIL-88A-1 and MIL-88A-2.

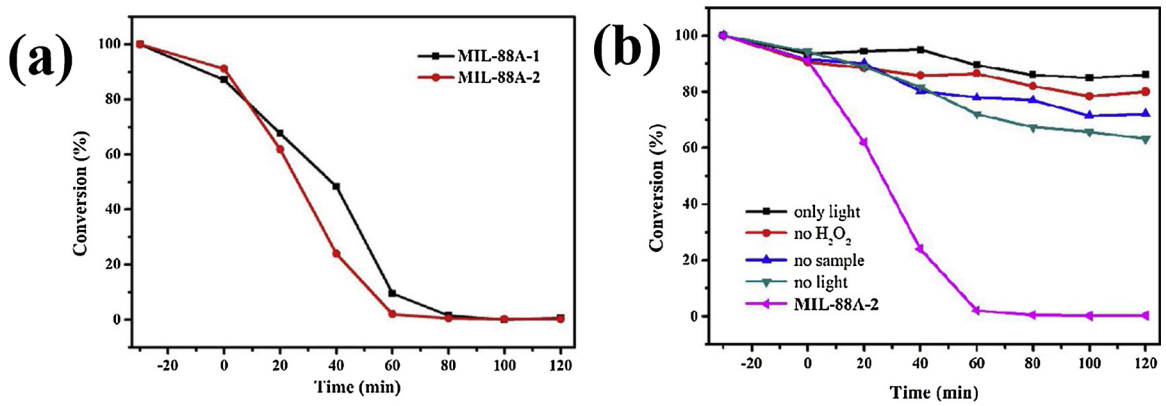

Fig. 3. (a) The degradation efficiency of RhB by MIL-88A-1 or MIL-88A-2 and (b) the comparative experiments of degradation of RhB by MIL-88A-2.

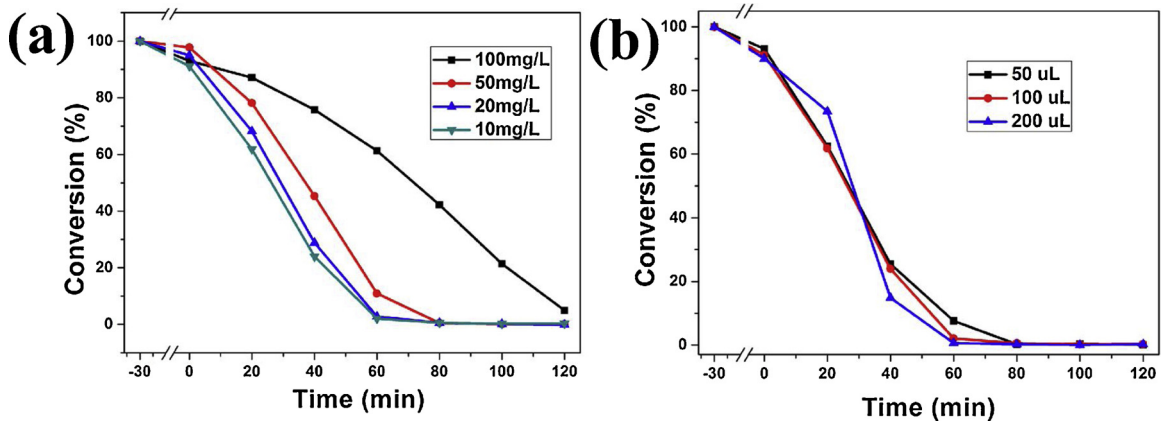

Fig. 4. The effect of (a) RhB concentration, (b) H_2O_2 dosage on degradation efficiency of MIL-88A-2.

that of the MIL-88A-1, which also could be due to its smaller size and larger active sites. Fig. 5b shows that self-degradation of BPA was about 2 % after 120 min irradiation under visible light, only 17 % degradation was realized just with the addition of MIL-88A-2, and only 25 % degradation was acquired just with H_2O_2. When both MIL-88A-2 and H_2O_2 were added under dark condition, 50 % degradation was acquired, while a markedly increase of the catalytic activity appeared under visible light irradiation in the presence of the MIL-88A-2 and H_2O_2. These results are similar to those of the RhB degradation.

Except for MOF-5, most MOFs belong to molecular photocatalysts, which could be described as highest occupied molecular orbital (HOMO) - lowest unoccupied molecular orbital (LUMO) theory. Upon the visible light irradiation, electron (e^-) is excited from HOMO to LUMO, leaving a hole (h^+) on the HOMO. The h^+ can react with H_2O_2 to form ·OH, and e^- can react with dissolved O_2 to form $\cdot O_2^-$. The h^+, ·OH and $\cdot O_2^-$ all could lead to the oxidation of organic pollutants. However, the photocatalytic degradation of RhB and BPA is limited in the absence of H_2O_2, as shown in Fig. 3b and b, which could be attributed to the rapid recombination of h^+ and e^-, and weak oxidative capacity of the h^+ and radicals. With the addition of H_2O_2 and MIL-88A-2 under dark condition, the degradation of RhB and BPA was increased (Fig. 3b and 5b), which could be attributed to the increase of ·OH as Fe-O clusters on the surface of the MIL-88A can activate H_2O_2 by Fenton-like reaction, which was described as Eq. (1) and (2). However, the increase of RhB and BPA degradation by Fenton-like catalysis is limited. Upon visible light irradiation, MIL-88A could generate h^+ and

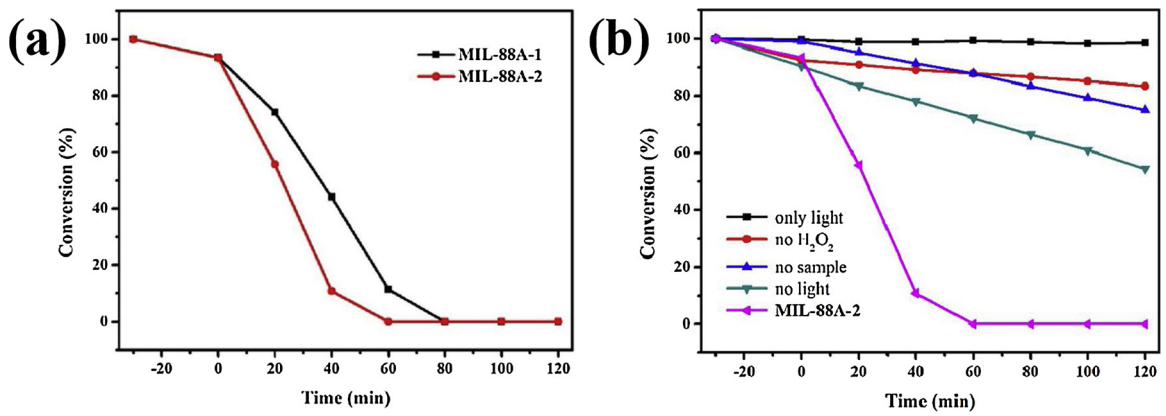

Fig. 5. (a) The degradation efficiency of BPA by MIL-88A-1 or MIL-88A-2 and (b) the comparative experiments of degradation of BPA by MIL-88A-2.

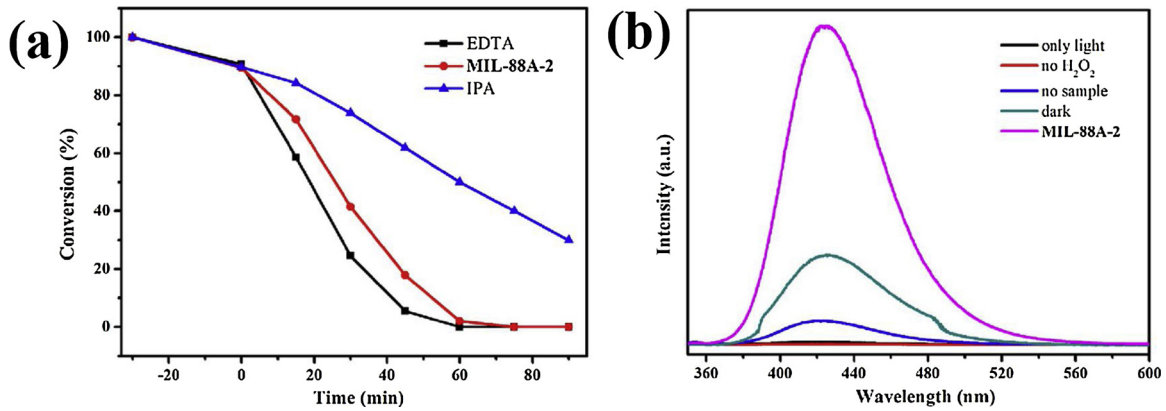

Fig. 6. (a) Effect of different scavengers on the degradation of RhB by MIL-88A-2, and (b) Fluorescence emission spectra of •OH radicals generated during the catalytic process at 315 nm on contrast experiments.

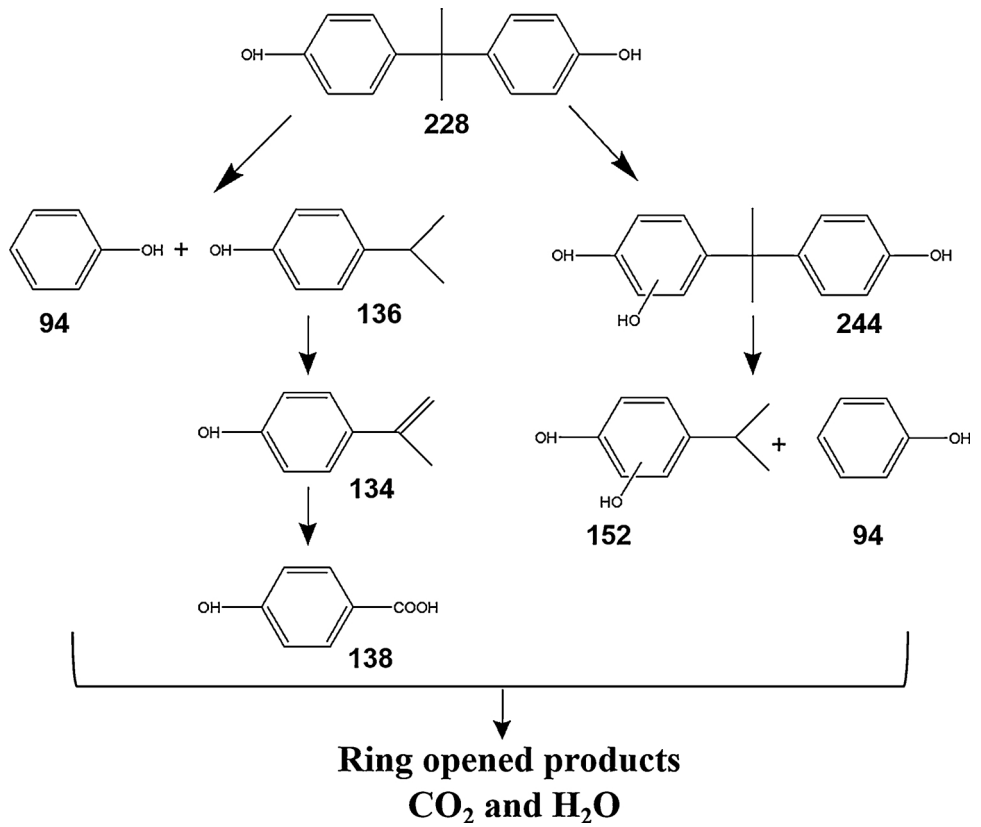

Fig. 7. The proposed pathway for the degradation of BPA.

e- through Eq. (3). H_2O_2, as the electron acceptor, can capture the e^- to form •OH radical, inhibiting the recombination of h^+ and e^- and finally the improving the RhB and BPA degradation, which was described as Eq. (4). From the above discussion, it can be concluded that the photo-Fenton reaction were the main mechanism for the degradation of RhB and BPA.

$$Fe^{3+} + H_2O_2 \rightarrow Fe^{2+} + \bullet HOO + H^+ \quad (1)$$

$$Fe^{2+} + H_2O_2 \rightarrow Fe^{3+} + \bullet OH + OH^- \quad (2)$$

$$\text{MIL-88A} + hv \rightarrow h^+ + e\text{-} \quad (3)$$

$$e^- + H_2O_2 \rightarrow \bullet OH + OH^- \quad (4)$$

To verify this mechanism, active species experiments were conducted. 0.5 mM EDTA and IPA were introduced to capture h^+ and •OH radical, respectively. As shown in Fig. 6a, the RhB degradation was greatly restricted after introduction of IPA. While, in the presence of EDTA, the RhB decomposition was improved because of the inhibition of the recombination of h^+ and e^-, and the enhancement of the formation of •OH. These results implied that the main active specie should be •OH radical. It is reported that the concentration of •OH radical can be determined by fluorescence method [54]. ·OH can be effectively and selectively trapped by terephthalic acid to form 2-hydroxy terephthalic acid that can emit fluorescence at 425 nm when excited at 315 nm, as reported in the literature [54,55], and the intensity of the peak at 426 nm is proportional to the concentration of the •OH radical. The experiment is similar to the photocatalytic process except that a solution of 0.5 mM terephthalic acid and 2 mM NaOH replace the RhB solution. After 30 min irradiation under visible light, some solution was extracted, and the fluorescence spectra was recorded on Techcomp FL970 fluorescence spectrometer with an excitation wavelength of

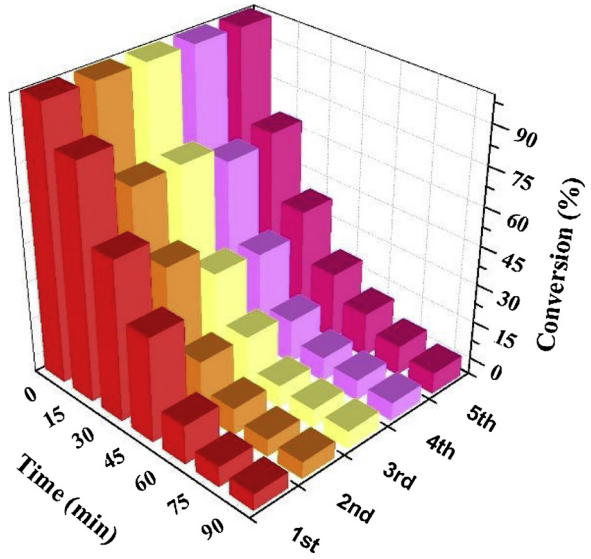

Fig. 8. The cyclic experiments of catalytic degradation of RhB over the MIL-88A-2.

315 nm. Fig. 6b indicates that there is no signal just with the addition of MIL-88A-2, implying that the photogenerated h^+ can't lead to the formation of •OH radical. A small peak appeared only with H_2O_2 under light irradiation, which means that the RhB degradation by the oxidation of H_2O_2 existed. An increase was found with the introduction H_2O_2 and MIL-88A-2 under dark condition, meaning that •OH radical generated through Eq. (1) and (2) played a role in the degradation of organic pollutants. The intensity of the PL peak increase greatly in the presence of H_2O_2 and MIL-88A-2 under visible light irradiation, suggesting the formation of more •OH radical and the improvement of the degradation efficiency. It corresponds well with the results of Fig. 3b and 5 b, further confirming the important role of •OH radical in the degradation process.

To understand the degradation pathway of BPA, LC—MS analysis was conducted to identify the intermediates. The possible oxidation products were identified (Table S1), and several possible degradation pathways were proposed, as shown in Fig. 7. The C—C bond of BPA between benzene rings and isopropyl was ruptured to generate phenol and 4-isopropylphenol that could be converted into 4-isopropenylphenol and 4-hydroxybenzoic acid [56–59]. The detected species with m/z = 244 could be monohydroxylated BPA that could further react with ·OH to cause the bond cleavages and produce the intermediates of isopropylhydroquinone and phenol [58–60]. These intermediates with low molecular weights would be further oxidized to ring opened products, and finally CO_2 and H_2O.

Reusability is a significant parameter to evaluate catalysts. RhB was selected as the target pollutant to study the reuse of the MIL-88A. After the first cycle, the MIL-88A-2 was centrifuged and re-dispersed in RhB solution, and it can be seen from Fig. 8 that there is no obvious decline of the degradation efficiency after five cycles. XRD pattern of MIL-88A-2 after catalytic experiment was shown in Fig. 9a. It can be seen that the diffraction pattern of the used MIL-88A-2 was similar to that of the as-prepared MIL-88A-2 washed with water, indicating the good stability of the MIL-88A. SEM image (Fig. 9b) show that the MIL-88A-2 after photo-Fenton degradation of RhB was similar to the as-prepared MIL-88A-2. Furthermore, XPS spectra (Fig. 9c), TGA curves (Fig. 9d) and EDS results (Table S2) of MIL-88A-2 were not changed obviously before and after photo-Fenton reaction, and the difference of the loss weight (Fig. 9d) could be attributed to the changes of the guest molecules in MIL-88A. These results suggested the good reusability and the long-term operation of the MIL-88A.

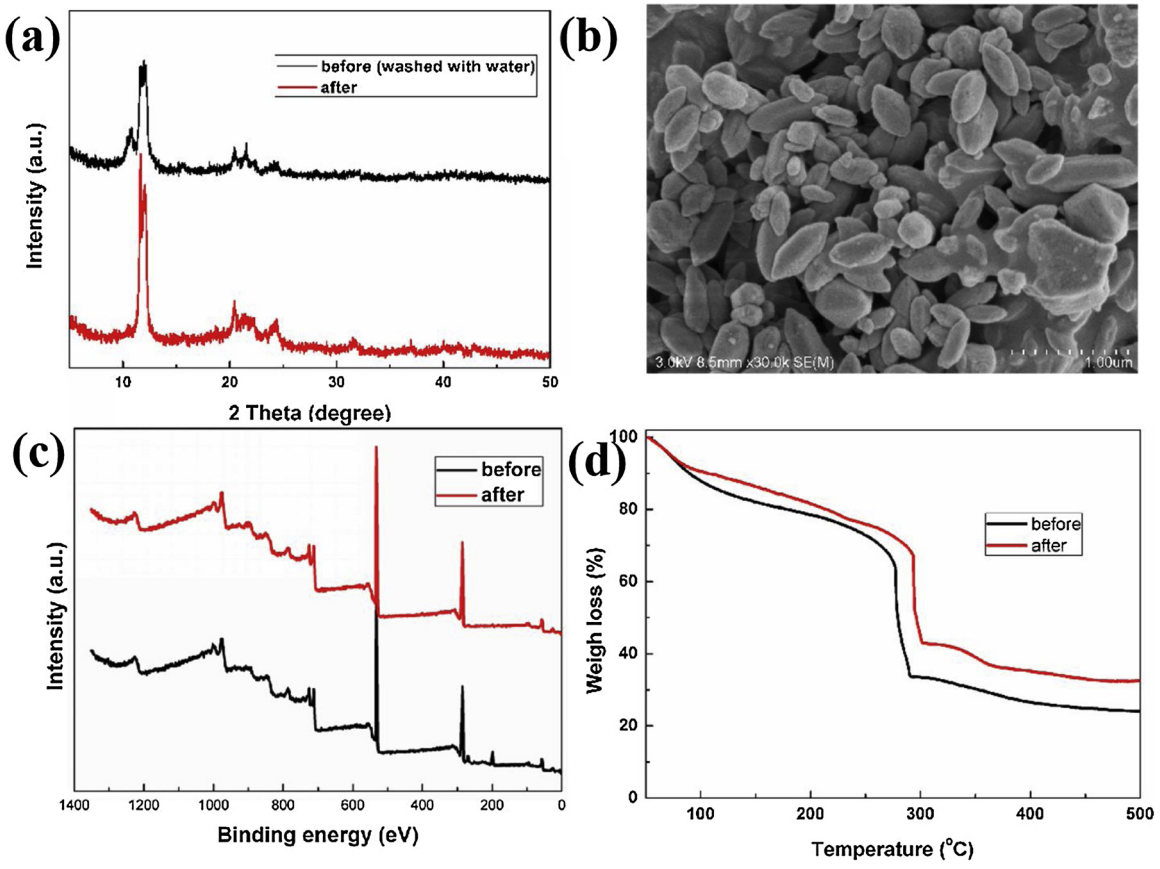

Fig. 9. (a) XRD patterns, (b) SEM image, (c) XPS spectra and (d) TGA curves of MIL-88A-2 before and after photo-Fenton reaction.

4. Conclusion

In conclusion, MIL-88A with different sizes was prepared successfully at room temperature. This method is green and facilitates the large-scale synthesis, which is imperative to push forward development of MIL-88A. During the preparation process, water played an important role as water could facilitate the deprotonation of fumaric acid and hydrolysis of iron salt to accelerate crystal nucleation. Both MIL-88A-1 and MIL-88A-2 exhibited excellent photo-Fenton catalytic degradation efficiency towards RhB and BPA in the presence of H_2O_2 under visible light, and MIL-88A-2 with smaller size had better photo-Fenton catalytic activity than MIL-88A-1. H_2O_2, as an electron acceptor, greatly improve the degradation of RhB and BPA, in which the main active specie was •OH generated from the reaction between e^- and H_2O_2, and the Fenton-like reaction. In addition, the as-synthesis MIL-88A possessed good reusability, and there was no obvious decline of the degradation efficiency after five cycles. This work taped a new door to produce MIL-88A under ambient temperature and mild condition, which will provide a new possibility for its large-scale application.

CRediT authorship contribution statement

Huifen Fu: Data curation, Investigation, Visualization, Writing - original draft. **Xiao-Xu Song:** Data curation, Methodology, Software. **Lin Wu:** Visualization, Software. **Chen Zhao:** Validation, Software. **Peng Wang:** Resources. **Chong-Chen Wang:** Conceptualization, Funding acquisition, Supervision, Project administration, Writing - review & editing.

Declaration of Competing Interest

The authors declare that they have no known competing financial interests or personal relationships that could have appeared to influence the work reported in this paper.

Acknowledgements

This work was supported by the National Natural Science Foundation of China (21806008, 21876008, 51878023, 51578034), Beijing Natural Science Foundation (8202016), Beijing Talent Project (2019A22), Great Wall Scholars Training Program Project of Beijing Municipality Universities (CIT&TCD20180323), Project of Construction of Innovation Teams and Teacher Career Development for Universities and Colleges Under Beijing Municipality (IDHT20170508).

Appendix A. Supplementary data

Supplementary material related to this article can be found, in the online version, at doi:https://doi.org/10.1016/j.materresbull.2020.110806.

References

[1] D. Awfa, M. Ateia, M. Fujii, M.S. Johnson, C. Yoshimura, Photodegradation of pharmaceuticals and personal care products in water treatment using carbonaceous-TiO_2 composites: a critical review of recent literature, Water Res. 142 (2018) 26–45.

[2] K.H. Chu, Y.A.J. Al-Hamadani, C.M. Park, G. Lee, M. Jang, A. Jang, N. Her, A. Son, Y. Yoon, Ultrasonic treatment of endocrine disrupting compounds, pharmaceuticals, and personal care products in water: a review, Chem. Eng. J. 327 (2017) 629–647.

[3] J. Hao, Q. Zhang, P. Chen, X. Zheng, Y. Wu, D. Ma, D. Wei, H. Liu, G. Liu, W. Lv, Removal of pharmaceuticals and personal care products (PPCPs) from water and wastewater using novel sulfonic acid (–SO_3H) functionalized covalent organic frameworks, Environ. Sci. Nano (2019), https://doi.org/10.1039/C9EN00708C.

[4] X.-Y. Xu, C. Chu, H. Fu, X.-D. Du, P. Wang, W. Zheng, C.-C. Wang, Light-responsive UiO-66-NH_2/Ag_3PO_4 MOF-nanoparticle composites for the capture and release of sulfamethaxazole, Chem. Eng. J. 350 (2018) 436–444.

[5] I.A. Vasiliadou, R. Molina, F. Martinez, J.A. Melero, Biological removal of pharmaceutical and personal care products by a mixed microbial culture: sorption, desorption and biodegradation, Biochem. Eng. J. 81 (2013) 108–119.

[6] M. Cai, R. Li, Z. Xie, J. Huang, Y. Zeng, Q. Zhang, H. Liu, W. Lv, G. Liu, Synthesis of a core-shell heterostructured MoS_2/$Cd_{0.9}Zn_{0.1}S$ photocatalyst for the degradation of diclofenac under visible light, Appl. Catal. B 259 (2019) 118033.

[7] Q. Zhang, P. Chen, M. Zhou, F. Wang, Y. Su, T. Chen, K. Yao, Z. Cai, W. Lv, G. Liu, Degradation of indometacin by simulated sunlight activated CDs-loaded $BiPO_4$ photocatalyst: roles of oxidative species, Appl. Catal. B 221 (2018) 129–139.

[8] S. Bagheri, A. TermehYousefi, T.-O. Do, Photocatalytic pathway toward degradation of environmental pharmaceutical pollutants: structure, kinetics and mechanism approach, Catal. Sci. Technol. 7 (2017) 4548–4569.

[9] S. Salamat, H. Younsei, N. Bahramifar, Synthesis of magnetic core–shell Fe_3O_4@TiO_2 nanoparticles from electric arc furnace dust for photocatalytic degradation of steel mill wastewater, RSC Adv. 7 (2017) 19391–19405.

[10] Z. Shayegan, C.-S. Lee, F. Haghighat, TiO_2 photocatalyst for removal of volatile organic compounds in gas phase-A review, Chem. Eng. J. 334 (2018) 2408–2439.

[11] S.-Y. Lee, S.-J. Park, TiO_2 photocatalst for water treatment applications, J. Ind, Eng. Chem. 19 (2013) 1761–1769.

[12] Y. Ohko, I. Ando, C. Niwa, T. Tatsuma, T. Yamamura, T. Nakashima, Y. Kubota, A. Fujishima, Degradation of biphenol A in water by TiO_2 photocatalyst, Environ. Sci. Technol. 35 (2001) 2365–2368.

[13] C.-Y. Wang, H. Fu, P. Wang, C.-C. Wang, Highly sensitive detect of p-arsanilic acid with a new water-stable europium metal-organic framework, Appl. Organometal. Chem. (2019) e5021.

[14] E. Chen, H. Yang, J. Zhang, Zeolitic imidazolate framework as formaldehyde gas sensor, Inorg. Chem. 53 (2014) 5411–5413.

[15] M. Yao, W. Tang, G. Wang, B. Nath, Gang Xu, MOF Thin film-coated metal oxide nanowire array: significantly improved chemiresistor sensor performance, Adv. Mater. 28 (2016) 5229–5234.

[16] Y. He, W. Zhou, G. Qian, B. Chen, Methane storage in metal-organic frameworks, Chem. Soc. Rev. 43 (2014) 5657–5678.

[17] M.P. Suh, H.J. Park, T.K. Prasad, D.-W. Lim, Hydrogen storage in metal-organic frameworks, Chem. Rev. 112 (2012) 782–835.

[18] Q. Yang, D. Liu, C. Zhong, J.-R. Li, Development of computational methodologies for metal-organic frameworks and their application in gas separations, Chem. Rev. 113 (2013) 8261–8323.

[19] J.-J. Li, H. Fu, J.-R. Cui, P. Xu, J. Guo, J.-R. Li, High-performance adsorption and separation of anionic dyes in water using a chemically stable graphene-like metal-organic framework, Dalton Trans. 46 (2017) 10197–11020.

[20] J. Li, X. Wang, G. Zhao, C. Chen, Z. Chai, A. Alsaedi, T. Hayat, X. Wang, Metal-organic framework-based materials: superior adsorbents for the capture of toxic and radioactive metal ions, Chem. Soc. Rev. 47 (2018) 2322–2356.

[21] R. Kaur, A. Kaur, A. Umar, W.A. Anderson, S.K. Kansal, Metal organic framework (MOF) porous octahedral nanocrystals of Cu-BTC: synthesis, properties and enhanced adsorption properties, Mater. Res. Bull. 109 (2019) 124–133.

[22] A. Morozan, F. Jaouen, Metal organic frameworks for electrochemical applications, Energy Environ. Sci. 5 (2012) 9269–9290.

[23] Y. Wen, J. Zhang, Q. Xu, X.-T. Wu, Q.-L. Zhu, Pore surface engineering of metal-organic frameworks for heterogeneous catalysis, Coord. Chem. Rev. 376 (2018) 248–276.

[24] C.-C. Wang, X.-H. Yi, P. Wang, Powerful combination of MOFs and C_3N_4 for enhanced photocatalytic performance, Appl. Catal. B 247 (2019) 24–48.

[25] Y. Lee, S. Kim, J.K. Kang, S.M. Cohen, Photocatalytic CO_2 reduction by a mixed metal(Zr/Ti), mixed ligand metal-organic framework under visible light irradiation, Chem. Commun. 51 (2015) 5735–5738.

[26] W. Mei, H. Song, Z. Tian, S. Zuo, D. Li, H. Xu, Efficient photo-Fenton like activity in modified MIL-53(Fe) for removal of pesticides: regulation of photogenerated electron migration, Mater. Res. Bull. 119 (2019) 110570.

[27] R. Liang, S. Luo, F. Jing, L. Shen, N. Qin, L. Wu, A simple strategy for fabrication of Pd@MIL-100(Fe) nanocomposite as a visible-light-driven photocatalyst for the treatment of pharmaceuticals and personal care products (PPCPs), Appl. Catal. B 176-177 (2015) 240–248.

[28] S. Li, J. Cui, X.Wu.X. Zhang, Q. Hu, X. Hou, Rapid in situ microwave synthesis of Fe_3O_4@MIL-100(Fe) for aqueous diclofenac sodium removal through integrated adsorption and photodegradation, J. Hazard. Mater. 373 (2019) 408–416.

[29] X. Chen, Y. Zhang, Y. Zhao, S. Wang, L. Liu, W. Xu, Z. Guo, S. Wang, Y. Liu, J. Zhang, Encapsulating Pt nanoparticles through transforming Fe_3O_4 into MIL-100 (Fe) for well-defined Fe_3O_4@MIL-100 (Fe) core-shell heterostructures with promoting catalytic activity, Inorg. Chem. 58 (2019) 12433–12440.

[30] X. He, H. Fang, D.J. Gosztola, Z. Jiang, P. Jena, W.-N. Wang, Mechanism insight into photocatalytic pathway of MIL-100(Fe)/TiO_2 composites, ACS Appl. Mater. Inter. 11 (2019) 12516–12524.

[31] Y. Gong, B. Yang, H. Zhang, X. Zhao, A g-C_3N_4/MIL-101(Fe) heterostructure composite for highly efficient BPA degradation with sulsufate under visible light irradiation, J. Mater. Chem. A 6 (2018) 23703–23711.

[32] Z. Zhang, X. Li, B. Liu, Q. Zhao, G. Chen, Hexagonal microspindle of NH_2-MIL-101(Fe) metal–organic frameworks with visible-light-induced photocatalytic activity for the degradation of toluene, RSC Adv. 6 (2016) 4289–4295.

[33] M. Li, J. Wang, Y. Zheng, Z. Zheng, C. Li, Z. Li, Anchoring NaYF4:Yb,Tm upconversion nanocrystals on concave MIL-53(Fe) octahedra for NIR-light enhanced photocatalysis, Inorg. Chem. Front. 4 (2017) 1757–1764.

[34] G. Chaturvedi, A. Kaur, S.K. Kansal, CdS-decorated MIL-53(Fe) microrods with enhanced visible light photocatalytic performance for the degradation of ketorolac tromethamine and mechanism insight, J. Phys. Chem. C 123 (2019) 16857–16867.

[35] J. Wang, J. Wan, Y. Ma, Y. Wang, M. Pu, Z. Guan, Metal–organic frameworks MIL-88A with suitable synthesis conditions and optimal dosage for effective catalytic

degradation of Orange G through persulfate activation, RSC Adv. 6 (2016) 112502–112511.
[36] Y. Li, J. Jiang, Y. Fang, Z. Cao, D. Chen, N. Li, Q. Xu, J. Lu, TiO_2 Nanoparticles anchored onto the metal–organic framework NH_2-MIL-88B(Fe) as an adsorptive photocatalyst with enhanced Fenton-like degradation of organic pollutants under visible light irradiation, ACS Sustainable Chem. Eng. 6 (2018) 16186–16197.
[37] S.G. Khasevani, N. Mohaghegh, M.R. Cholami, Kinetic study of navy blue photocatalytic degradation over Ag_3PO_4/$BiPO_4$@MIL-88B(Fe)@g-C_3N_4 core@shell nanocomposite under visible light irradiation, New J. Chem. 41 (2017) 10390–10396.
[38] Y. Guo, Z. Jia, Q. Shi, Z. Liu, X. Wang, L. Li, Zr (IV)-based coordination porous materials for adsorption of Copper(II) from water, Micropor. Mesopor. Mat. 285 (2019) 215–222.
[39] Y. Fu, H. Yang, R. Du, G. Tu, C. Xu, F. Zhang, M. Fan, W. Zhu, Enhanced photocatalytic CO_2 reduction over Co-doped NH_2-MIL-125(Ti) under visible light, RSC Adv. 7 (2017) 42819–42825.
[40] M. Díaz-García, Á. Mayoral, I. Díaz, M. Sánchez-Sánchez, Nanoscale M-MOF-74 materials prepared at room temperature, Cryst. Growth Des. 14 (2014) 2479–2487.
[41] J.Yan.Y. Yu, J. Xiao, Y. Li, Z. Li, Improved ethanol adsorption capacity and coefficient of performance for adsorption chillers of Cu-BTC@GO composite prepared by rapid room temperature synthesis, Ind. Eng. Chem. Res. 55 (2016) 11767–11774.
[42] X. Liao, F. Wang, F. Wang, Y. Cai, Y. Yao, B.-T. Teng, Q. Hao, S. Lu, Synthesis of (100) surface oriented MIL-88A-Fe with rod-like structure and its enhanced Fenton-like performance for phenol removal, Appl. Catal. B 259 (2019) 118064.
[43] N. Liu, W. Huang, X. Zhang, L. Tang, L. Wang, Y. Wang, M. Wu, Ultrathin graphene oxide encapsulated in uniform MIL-88A(Fe) for enhanced visible light-driven photodegradation of RhB, Appl. Catal. B 221 (2018) 119–128.
[44] J. Amaro-Gahete, R. Klee, D. Esquivel, J.R. Ruiz, C. Jiménez-Sanchidrián, F.J. Romero-Salguero, Fast ultrasound-assisted synthesis of highly crystalline MIL-88A particles and their application as ethylene adsorbents, Ultrason. Sonochem. 50 (2019) 59–66.
[45] C. Mellot-Draznieks, C. Serre, S. Surble, N. Audebrand, G. Ferey, Very large swelling in hybrid frameworks: a combined computational and powder diffraction study, J. Am. Chem. Soc. 127 (2005) 16273–16278.
[46] X.-X. Song, H. Fu, X. Li, X.-H. Yi, H.-Y. Chu, C.-C. Wang, Facile and rapid preparation of ZnO nanomaterials with different morphologies and superficial structures for enhanced ethanol sensing performances, J. Inorg. Organomet. P. 29 (2019) 33–40.
[47] Y. Zhang, J. Zhou, X. Chen, L. Wang, W. Cai, Coupling of heterogeneous advanced oxidation processes and photocatalysis in efficient degradation of tetracycline hydrochloride by Fe-based MOFs : synergistic effect and degradation pathway, Chem. Eng. J. 369 (2019) 745–757.
[48] K.-Y. Lin, H.-A. Chang, C.-J. Hsu, Iron-based metal organic framework, MIL-88A, as a heterogeneous persulfate catalyst for decolorization of Rhodamine B in water, RSC Adv. 5 (2015) 32520–32530.
[49] T. He, B. Ni, X. Xu, H. Li, H. Lin, W. Yuan, J. Luo, W. Hu, X. Wang, A competitive coordination strategy to finely tune pore environment of zirconium-based metal-organic frameworks, ACS Appl. Mater. Inter. 9 (2017) 22732–22738.
[50] T. He, X. Xu, B. Ni, H. Wang, Y. Long, W. Hu, X. Wang, Fast and scalable synthesis of uniform zirconium, hafnium-based metal-organic framework nanocrystals, Nanoscale 9 (2017) 19209–19215.
[51] W.-T. Xu, L. Ma, F. Ke, F.-M. Peng, G.-S. Xu, Y.-H. Shen, J.-F. Zhu, L.-G. Qiu, Y.-P. Yuan, Metal–organic frameworks MIL-88A hexagonal microrods as a new photocatalyst for efficient decolorization of methylene blue dye, Dalton Trans. 43 (2014) 3792–3798.
[52] S.G. Khasevani, M.R. Gholami, Engineering a highly dispersed core@shell structure for efficient photocatalysis: A case study of ternary novel BiOI@MIL-88A(Fe)@g-C3N4 nanocomposite, Mater. Res. Bull. 106 (2018) 93–102.
[53] C.-W. Tsai, E.H.G. Langner, The effect of synthesis temperature on the particle size of nano-ZIF-8, Micropor. Mesopor. Mat. 221 (2016) 8–13.
[54] V.K. Sharma, M. Feng, Water depollution using metal-organic frameworks-catalyzed advanced oxidation processes: a review, J. Hazard. Mater. 372 (2019) 3–16.
[55] H.-P. Jing, C.-C. Wang, Y.-W. Zhang, P. Wang, R. Li, Photocatalytic degradation of methylene blue in ZIF-8, RSC Adv. 4 (2014) 54454–54462.
[56] H. Katsumata, S. Kawabe, S. Kaneco, T. Suzuki, K. Ohta, Degradation of bisphenol A in water by the photo-Fenton reaction, J. Photoch. Photobio. A 162 (2004) 297–305.
[57] R. Das, G. Li, B. Mai, T. An, Spore cells from BPA degrading bacteria Bacillus sp. GZB displaying high laccase activity and stability for BPA degradation, Sci. Total Environ. 640-641 (2018) 798–806.
[58] J. Liu, F. Xie, R. Li, T. Li, Z. Jia, Y. Wang, Y. Wang, X. Zhang, C. Fan, TiO_{2-x}/$AgPO_4$ photocatalyst: oxygen vacancy dependent visible light photocatalytic performance and BPA degradative pathway, Mat. Sci. Semicon. Proc. 97 (2019) 1–10.
[59] Wanpeng Liu, Honghua Zhang, Beipei Cao, Kunde Lin, Jay Gan, Oxidative removal of bisphenol A using zero valent aluminumeacid system, Water Res. 45 (2011) 1872–1878.
[60] B. Darsinou, Z. Frontistis, M. Antonopoulou, I. Konstantinou, D. Mantzavinos, Sono-activated persulfate oxidation of bisphenol A: kinetics, pathways and the controversial role of temperature, Chem. Eng. J. 280 (2015) 623–633.